**PAPER**

# Completion of the first ITER toroidal field coil structure

View the article online for updates and enhancements.

# Completion of the first ITER toroidal field coil structure

**M. Nakahira**[1] , **M. Iguchi**[1]**, T. Sakurai**[1]**, H. Ozeki**[1]**, E. Fujiwara**[1]**, K. Takano**[1]**,
Y.S. Hong**[1]**, M. Ino**[1]**, N. Koizumi**[1]**, N. Sawa**[2]**, D. Hara**[2]**, T. Inagaki**[2]**, S.Y. Kim**[3]**,
J.H. Choi**[3]**, S.S. Hwang**[3] **and C. Luongo**[4]

[1] National Institutes for Quantum and Radiological Science and Technology (QST), Chiba-shi, Japan
[2] Mitsubishi Heavy Industries Ltd, Kobe, Japan
[3] Hyundai Heavy Industries, Ulsan, Republic of Korea
[4] ITER Organization (IO), St. Paul-lez-Durance Cedex, France

E-mail: nakahira.masataka@qst.go.jp

## Abstract

The first ITER toroidal field coil structures (TFCS) have been successfully completed by the Japan Domestic Agency with the solving of major technical challenges, and further fabrication is ongoing. There were five major challenges for the TFCS fabrication. This paper describes these challenges and the solutions established during fabrication and how to implement to the ITER TFCS.

## 1. Introduction

This paper reports the completion of the first of 19 ITER toroidal field coil structures (TFCSs), the procurement responsibility of which is 100% that of the Japan Domestic Agency (JADA). The major technical challenges of the TFCSs of ITER are: (i) the development of new materials having high ductility under cryogenic temperatures (4 K), (ii) application of partial penetration welding (PPW), (iii) welding deformation control, (iv) development of specialized ultrasonic testing (UT) that factors in attenuation from austenitic stainless-steel weldments and (v) fitting the large (16 m × 9 m) complex D-shaped structure for closure welding (CW) within tolerances of 0.5 mm. Only by developing solutions for the respective challenges was the first ITER TFCS successfully completed.

The ITER TFCSs are massive 16 m × 9 m welded structures made of austenitic stainless steel that encase the superconducting toroidal field (TF) coils winding pack (WP) with a final closure weld, which requires extremely precise dimension-controlled structures to fit the closure weld root. The TFCSs must also support the weight and electromagnetic forces of the TF coils and be highly ductile at cryogenic temperatures of 4 K to retain structural integrity during

superconducting operation. A TFCS consists of four sub-assemblies (AU, AP, BU and BP), as shown in figure 1.

## 2. Fabrication of ITER TFCS

### 2.1. Challenge (i): material development

JADA has developed cryogenic structural material for the fusion experimental reactor for 30 years [1]. ITER superconducting coils have to ensure huge magnetic force in a cryogenic environment. High stress is generated in the inner leg of the TFCS, and the maximum static stress intensity is about 667 MPa [2]. To maintain high ductility at cryogenic temperatures, a special austenitic stainless steel with more than 1000 MPa of yield strength and more than 200 MPam$^{0.5}$ of fracture toughness ($K_{IC}$) at a temperature of 4 K was developed (JJ1 (C1)) [3]. JADA determined the correlation between yield strength at 4 K and C+N contents from the large amount of experimental data [4]. It can control yield strength by designing the C+N contents. Applying this knowledge, JADA also prepared three grades (C2:900, C3:700, C4:500 MPa yield strength at 4 K) of standard high-strength austenitic stainless steel 316LN. They are used depending on the required strength. JADA has a responsibility to procure such
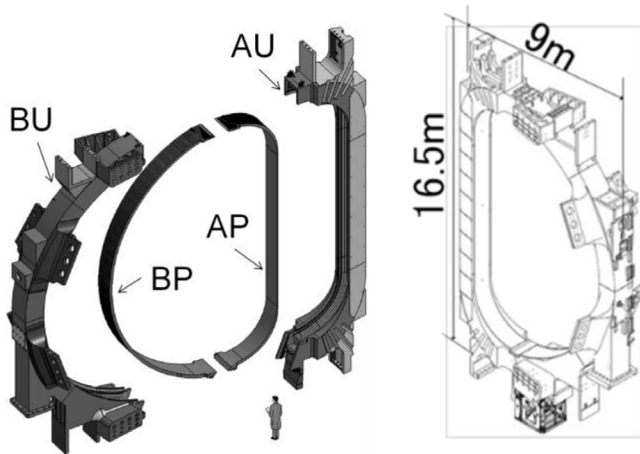
**Figure 1.** The ITER TF coil structure.

a special material of about 5000 ton while maintaining high quality. At the beginning of 2018, material procurement for the TFCS was completed.

Generally, the prospection of the fracture toughness with high accuracy was not developed enough. With such a background, JADA has secured the specification of fracture toughness by: (1) using only a qualified supplier; (2) checking using the Charpy impact test; and (3) sampling inspections. To improve the control parameters for fracture toughness, JADA performed surface observations, and after testing test pieces and investigating large amounts of sampling inspection data and additional trials, JADA discovered the strong correlation between Md30 and $K_{IC}$ at 4 K of material for the ITER TFCS (figure 2) [5]. Md30 is an existing parameter defined as the temperature at which 50% martensitic transformation occurs when 0.3 strain is applied [6]. Originally, it is a parameter to show tendency of martensitic transformation. It is a new finding to recognize the correlation between the Md30 and $K_{IC}$. One benefit of the Md30 is that it can be calculated from only chemical composition and grain size [7]. As a validation, JADA confirmed that high $K_{IC}$ material can be manufactured by controlling the Md30 [5]. The Md30 value control has been implemented as the scale of the sampling in the material procurement, which has improved the standard of quality.

### 2.2. Challenge (ii): PPW

The TFCSs have support attachments of PF and correction coils, some of which require PPW or fillet welding (FW). The PPW and FW joints have an unwelded area at the back side of the weld root, which is regarded as an as-weld notch with high stress concentration. During ITER operation, this as-weld notch takes static and cyclic loads at cryogenic temperature. However, since there was no specific design procedure for PPW and FW joints at cryogenic temperature, a design assessment process and non-destructive examination (NDE) method had to be established to verify structural integrity.

At first, fatigue crack growth (FCG) behaviour and properties were confirmed [8]. The compact tension (CT) specimens were prepared from a mock-up of the actual joint shape of the PPW, double J-groove (figure 3(a)). The specimens are

those with an as-weld notch (figure 3(b)) and those with an electronic discharge machining (EDM) notch with 0.2 mm diameter at the tip, the configurations of which are shown in figures 3(c), (c-1) and (c-2). FCG ratio (FCGR) tests were carried out under load control conditions with a stress ratio of 0.1 and target initial $\Delta K$ of 28 MPam$^{0.5}$. From the test results, it was decided to apply a fracture mechanic assessment to the design process, because cracks in the CT specimen with the as-weld notch grew from just after the start of the FCGR test, but one with an EDM notch needed a longer cycle to start crack growth. In addition, it could be said that; (1) since the cracks in all the CT specimens grew in weld metal, crack propagation analysis in weld metal was enough (figure 4(a)), and (2) properties of Paris's law obtained from these FCGR tests were able to be applied for FCG analysis (figure 4(b)).

Design by analysis was carried out by finite element (FE) models covering all the 133 weld joints applying the above FCGR test results. As the result of FE analyses, allowable initial defect sizes were defined for each weld joint to keep structural integrity during ITER operation. The minimum defect size to be detected in PPW/FW is 100 mm$^2$ of semi-elliptical at the root of the partial penetration weld, with an initial aspect ratio of 3 (4.6 mm of the minor radius, 13.8 mm of the major radius).

Because of accessibility and workability, the UT method is applied as NDE for PPW joints. To confirm detectability of UT in PPW joints, a UT verification test using a mock-up with a PPW joint was carried out. From this verification test result, it was shown that the conventional UT method according to ISO standards can measure welding depth with ± 1 mm accuracy. Based on this result, a UT procedure for PPW was defined that measured the PPW joint depth, compared the design depth, calculated the difference from the design and compared acceptable sizes for the depth and length obtained by scanning distance. For FW, a progressive die penetrant test (PPT) is applied as an alternative NDE method of UT, in which PT is applied to the first welding layer and to each of the three welding layers.

To establish the design assessment process for PPW at cryogenic temperatures, FCG behaviour and properties of the actual material with an as-weld notch had to be confirmed. In addition, the NDE method for PPW and FW joints to detect minimum allowable defects had to be developed. To solve them, JADA clarified the FCG behaviour of PPW under cryogenic temperature using a CT specimen prepared from a mock-up with an actual PPW joint, and established the NDE method by verifying the detectability of the PPW joint. These activities have been completed successfully. According to these establishments, JADA has completed design assessments for all PPW and FW joints.

### 2.3. Challenge (iii): welding deformation control

Particular attention must be given to the welds of the TFCS to confirm structural integrity at cryogenic temperatures and to control welding deformations. JADA performed welding qualification using mock-ups. Test pieces were sampled
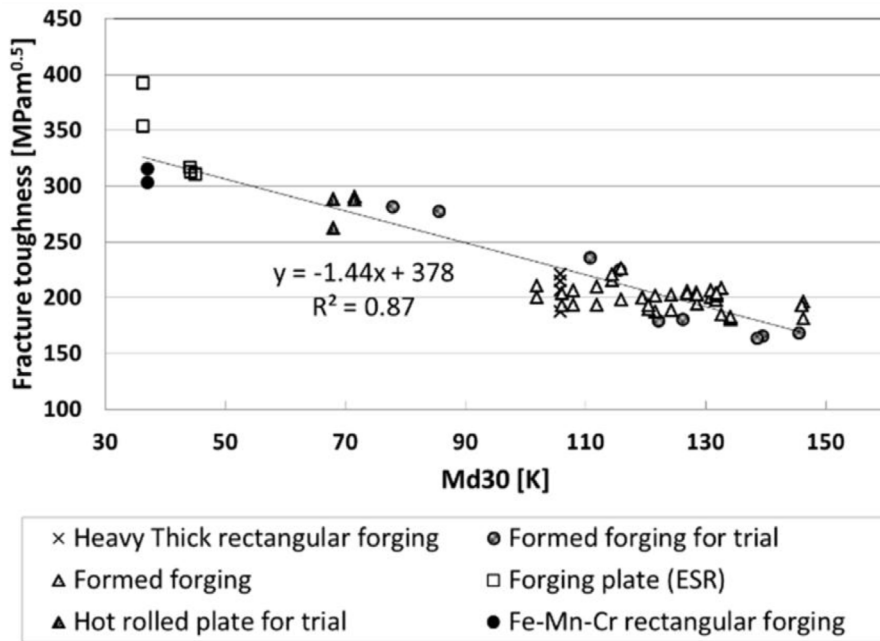
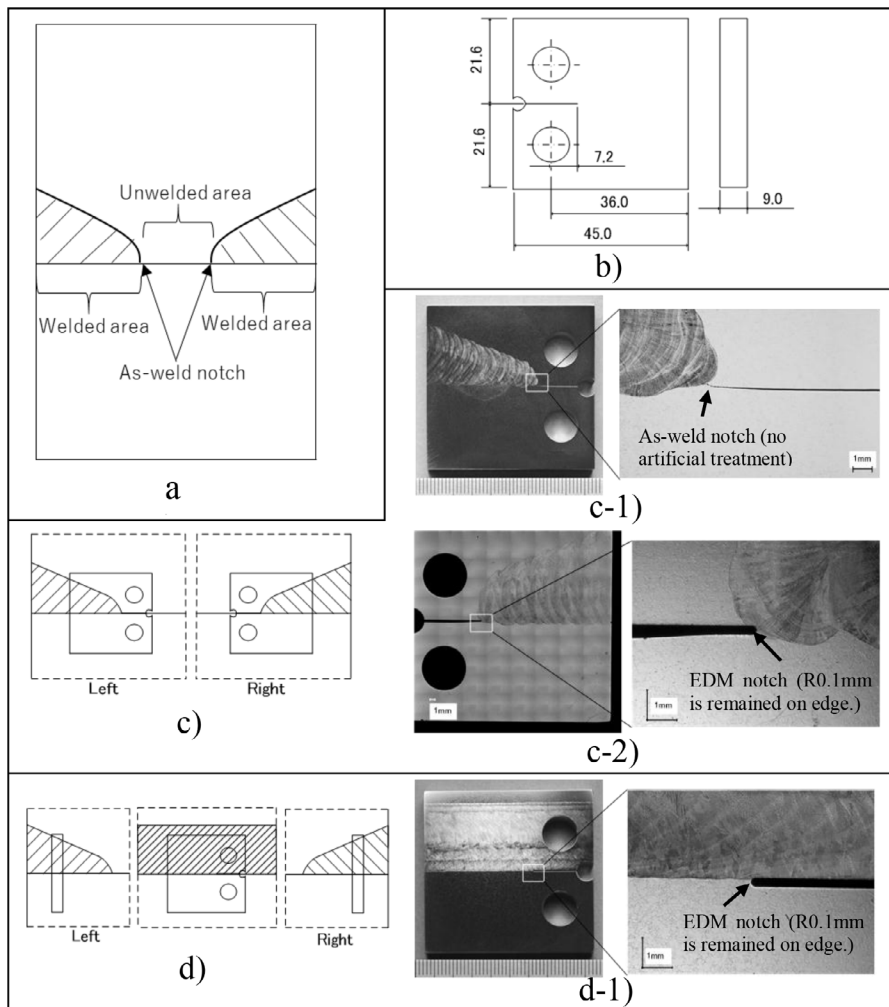**Figure 2.** The correlation between the fracture toughness and $Md_{30}$.



**Figure 3.** Information for mock-up and CT specimens: (*a*) an illustration of a mock-up with an actual PPW joint shape, (*b*) the dimensions of the CT specimen, (*c*) the sampling position of CT specimens for the as-weld and EDM notch (EDM dia. 0.2 mm applied to the as-weld notch and finally R 0.1 mm is remaining on the edge), (*c*-1) a photograph of a CT specimen with an as-weld notch, (*c*-2) a photograph of a CT specimen replacing the as-weld notch with an EDM notch, (*d*) the sampling position of CT specimens for weld metal, (*d*-1) a photograph of a CT specimen for weld metal.
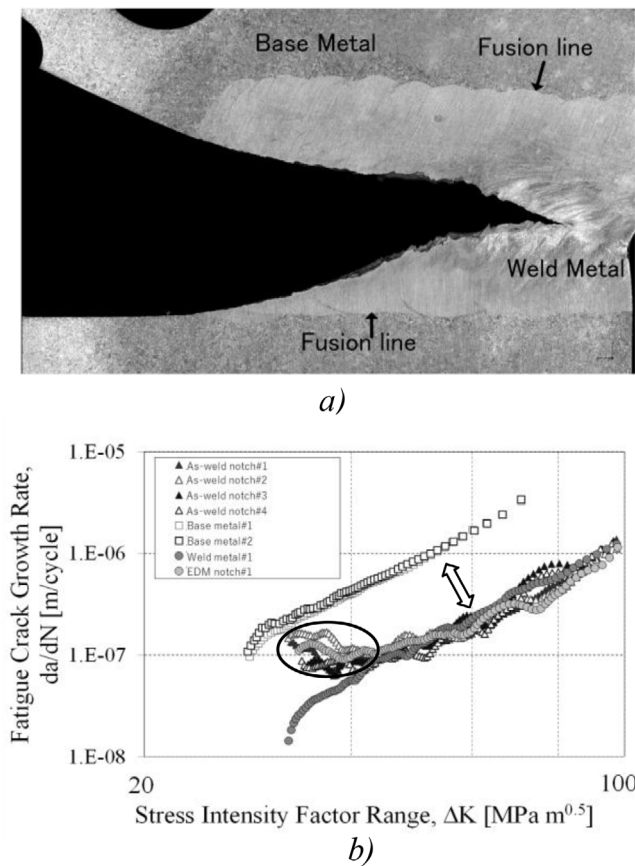
**Figure 4.** The FCGR test result: (*a*) a photographic overview of the as-weld notch type after the FCG test with etching by aqua regia, (*b*) the FCGR test results for all specimens.

from these mock-ups, and mechanical properties, such as fracture toughness and yield strength, were checked at cryogenic temperatures [9–11]. The mechanical properties of the welding joints also satisfy ITER requirements (YS > 500, 700, 900 and 1000 MPa, $K_{IC}$ > 180 MPa·m$^{0.5}$).

TFCSs consist of four sub-assemblies (SAs), which are called AU, BU, AP and BP. Because SAs are too large, JADA manufactures them in units of basic segments (BS) and welds segment-to-segment. An AU consists of three BSs and a BU consists of four BSs. A U-shape is formed from welding one outer plate and two side plates. Welding deformation was controlled by using a special welding process to compensate for angular distortion [9, 11, 12]. Segment-to-segment welding proved the most difficult because unlike flat plate welding, the complex U-shape makes angular distortion difficult to estimate. JADA performed a segment-to-segment (A1+A2) welding trial, and the amount of welding deformation and tendency of the welding direction were determined [13, 14]. Figure 5 shows an example of the segment-to-segment welding configuration using controlled deformation. Since the outer plate is quite thick and governs the angular distortion, this plate has a double groove for welding on both the inside and outside. The angular distortion was controlled by changing the welding deposit of the inside and outside of the thick outer plate. For example, the outside of the outer plate deposit deforms A1 toward the minus direction, and the inside of this deforms A1 to the plus direction. The side plates were

welded to keep the deposit heights the same as each other. A1 is initially offset from the result of the trial and deforms toward the reference line.

Figure 6 shows a controlled deformation for the first actual AU with respect to the deposit height of the sum of two side plates, and each deposit height of the inside and outside of the thick outer plate. The initial offset was approximately 4 mm and the gap from the reference line was controlled to be within a +2 mm margin, as deformation beyond the reference line was prohibited.

### 2.4. Challenge (iv): ultrasonic test

Since the coil case is a large-sized welded structure, the reliability of the volumetric examination that guarantees the welding quality is important for securing structural integrity.

Where radiographic examination is difficult due to the size of the coil case, ultrasonic examination is used. The longitudinal wave is selected, which is generally used for austenitic stainless-steel welds. There is concern that the signal level will decrease due to attenuation, because the ultrasonic wave propagates through the weld metal of austenitic stainless steel over a long distance. The attenuation of the UT beam in the weld is compensated by the transfer correction factor obtained from welding a test piece made of the actual TFCS material and weld metal during calibration.

Figure 7 shows the concept of weld attenuation calibration. Ultrasonic examination is performed using a distance amplitude characteristic (DAC) curve obtained by a calibration block made from base material of the TFCS with side drill holes (SDHs). Considering the sensitivity difference between the base material and weld material, signals obtained with a reference block made from a welding joint of the TFCS with the same SDHs in the weld are plotted on the DAC curve. The sensitivity difference is obtained from the difference between the signal level on the DAC and the plot. Finally, the relationship between the sensitivity difference and distance propagating in the weld metal is obtained. The sensitivity difference is used for assessment of the UT signal level to correct for decreasing by the weld metal by selecting the appropriate sensitivity difference with respect to the distance propagating in the weld metal in the actual UT.

Figure 8 shows the test results obtained by manufacturing companies. It was confirmed that the sensitivity difference (*y*) has a positive linear correlation as '$y = ax$' with the propagation distance (*x*) in the weld metal.

### 2.5. Challenge (v): fitting test

The TFCS is made of four SAs that will be welded together to constitute the TFCS only in the presence of the WP. It has to be checked that the tolerances are respected before this insertion. This is the objective of the fitting tests, associated with final machining.

The final machining of the TFCS was performed along the weld bevel for AU-AP, BU-BP and AU-BU with a gap and misalignment tolerance between two welding edges of around 0.5 mm, which required precise temperature control/
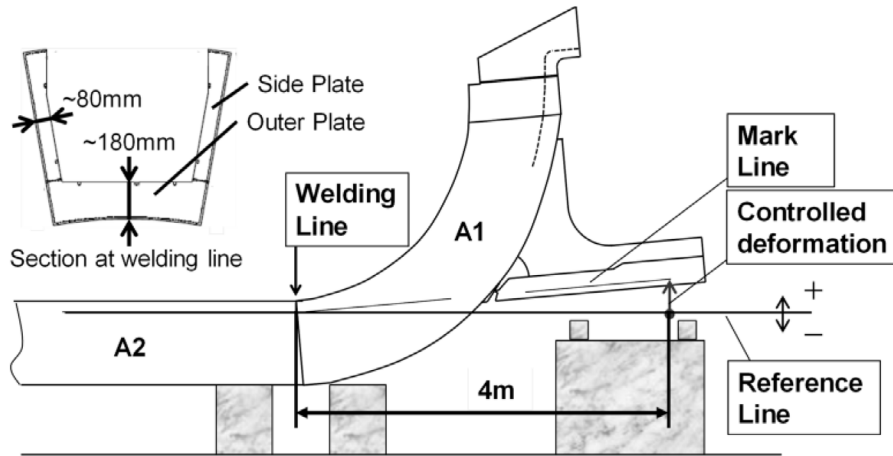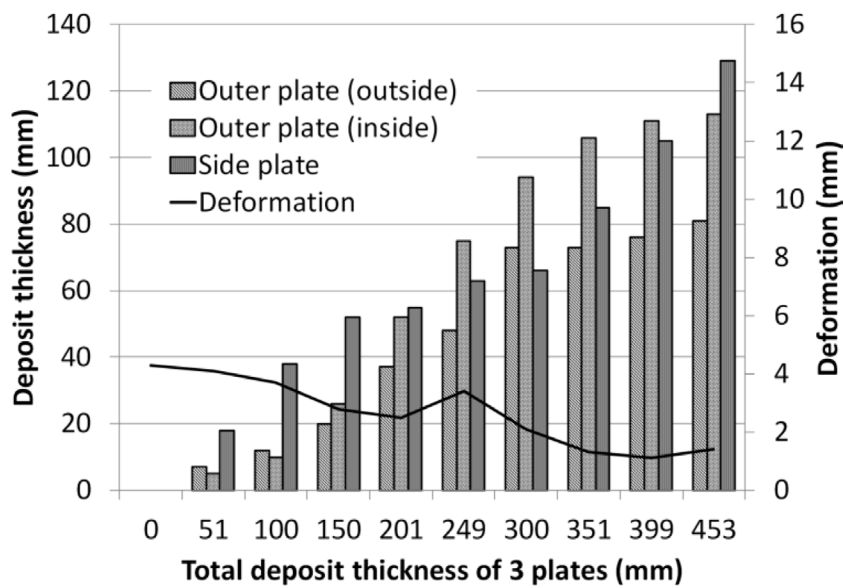
**Figure 5.** Segment-to-segment welding (A1–A2).



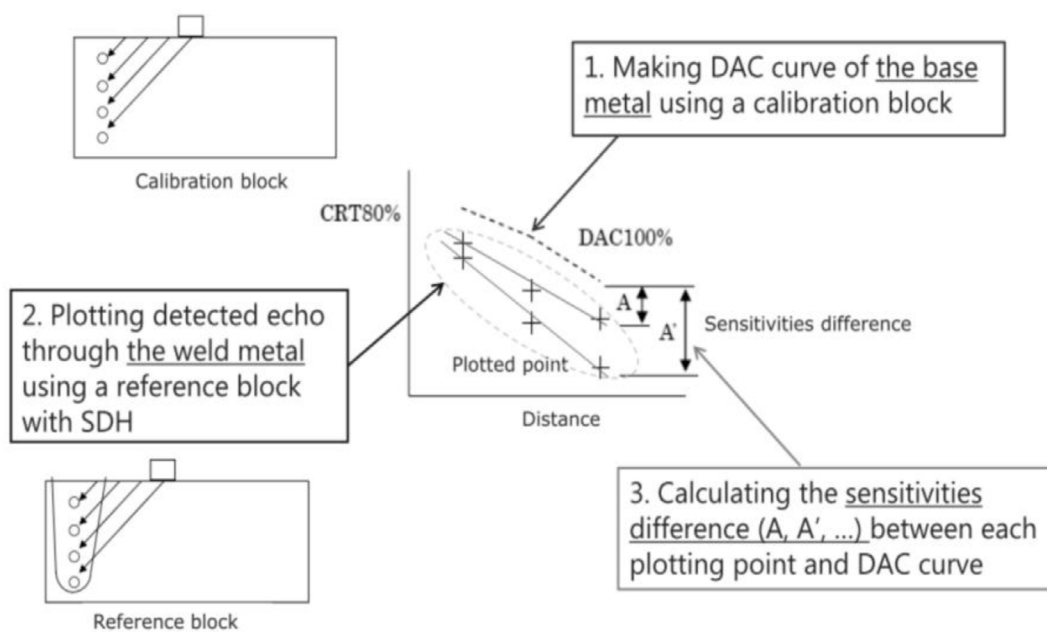**Figure 6.** An example of welding deformation.



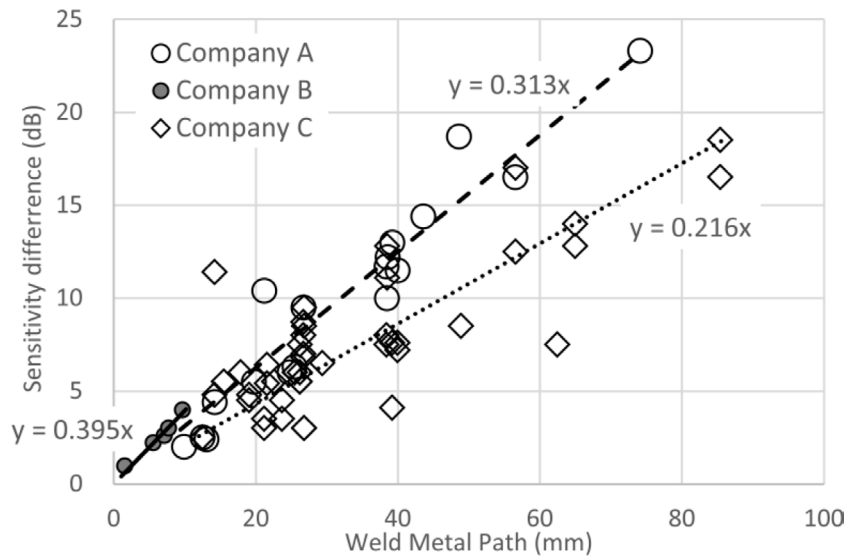**Figure 7.** The concept of the sensitivity setting for attenuation by weld metal.

5

**Figure 8.** Sensitivity difference by the propagation distance through weld metal.
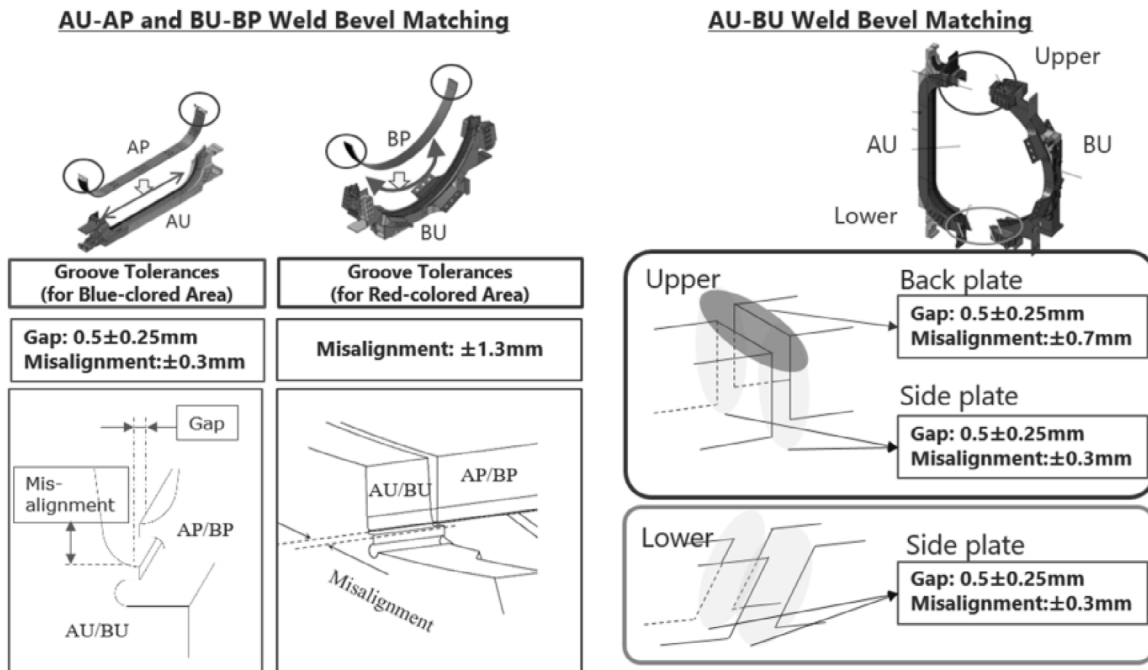


**Figure 9.** Weld root matching tolerances of the TFCS.

compensation. Figure 9 shows the tolerances of the weld bevel matching. The tolerance for the gap is $0.5 \pm 0.25$ mm. For the misalignment, the tolerance is $\pm 0.7$ mm for the back plate of the U-shape, and $\pm 0.3$ mm for its side plates. The final machining of the weld bevels on the SAs were performed by three different companies using several different machines under a temperature controlled environment within $20 \pm 5°$ Celsius as a target, or by applying a detailed temperature correction factor obtained on the machine to perform the final machining to avoid their mismatch due to thermal expansion. In addition, custom machining was applied to the weld bevel on BU reflecting the actual AU bevel position measurement

data. As a key activity to ensure the structural integrity, fitting tests of weld bevels with actual AU and AP, BU and BP, and AU and BU were performed after the final machining and the following dimensional survey.

Two types of fitting test methods are performed: one is for the AU and AP tests, as shown in figure 10, and for the BU and BP tests. The other is for the AU and BU tests, as shown in figure 11. In the former case, AU or BU was fixed on the ground to allow AP or BP to access slowly from the upper side. The difficulty is to control not only the precise position of AP and BP but also the flexibility of them, which causes a shape change during operation. Several types of guide jigs for
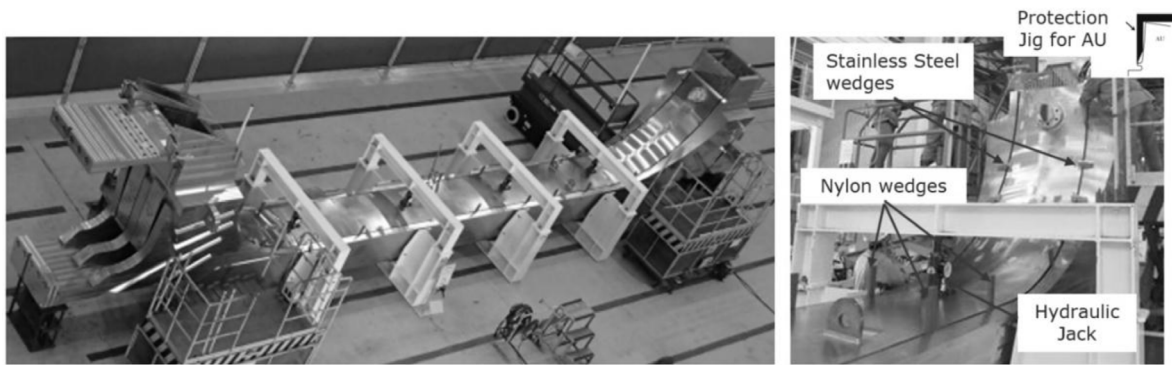
**Figure 10.** The AU-AP fitting test (left) and guide jigs to control the position of AP (right).



(a)

(b)
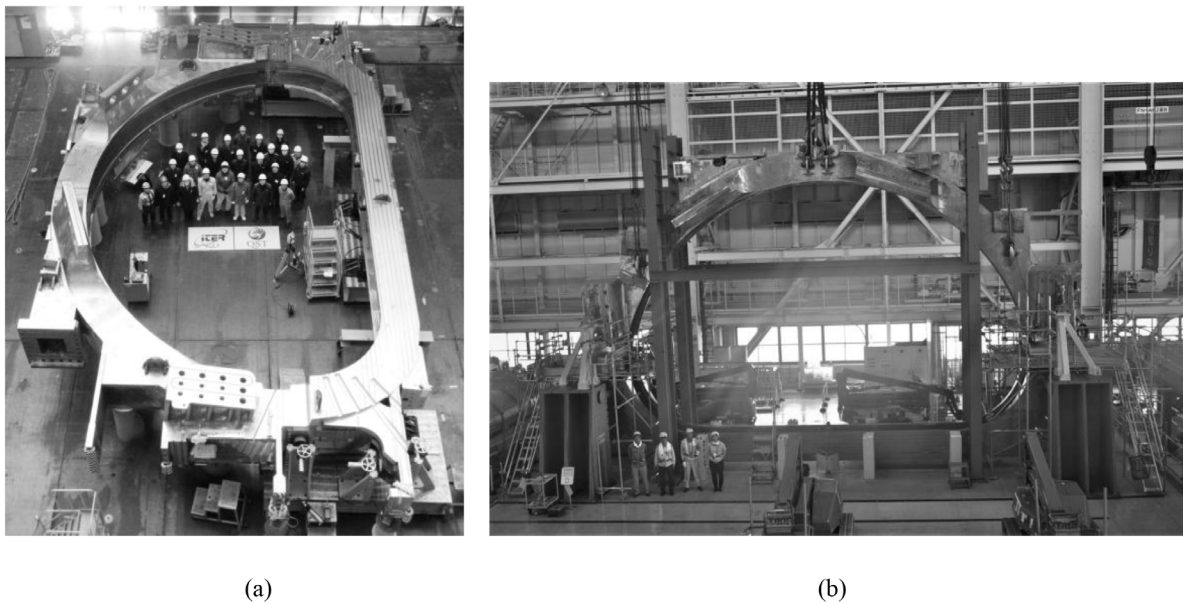
**Figure 11.** The first completion of the AU and BU fitting test: (*a*) EU01 fitting test. (*b*) JA01 fitting test.

AP and BP are shown in figure 10 to adjust them to AU and BU welding bevels. Eventually both tests were successfully completed.

In the AU and BU fitting tests, both were laid down on the ground for EU01. Here, BU was fixed on the floor, while AU was set on the rail guide. Then, AU was slid toward BU to match the bevel surface of the weld grooves. On the other hand, AU was set on the floor and BU was lifted down toward AU for JA01. In this case, the BU position was adjusted using jacks with respect to jigs attached on AU.

The difficulty of this test was to find the exact position of AU and BU to achieve the target criteria. Thus, before the actual work of fitting-up, virtual fitting based on the dimension survey data of AU and BU was performed. The result of the virtual fitting successfully provided the position of AU and BU, satisfying the target criteria of the welding root fitting. The actual fitting test was performed by monitoring the actual relative AU position to BU using a laser tracker. In the results of the fitting test, it was found that most of the weld root fitted within the tolerances of the gap and misalignment. The rest of the part was slightly out of the tolerance. However, it was judged that the welding could still be applicable since the deviation was small enough. Finally, the manufacturing of all the AU, AP, BU and BP of the first product set was completed.

## 3. Conclusion

The ten TFCSs will be delivered to the EU to be assembled with ten EU WPs, and nine TFCSs will be assembled in Japan with nine JA WPs. One spare TFC is included in the JA TF coil procurement. The first TFCS was delivered to the EU in March 2018 and the second TFCS was delivered in July 2018 for assembly with the EU-manufactured WP to complete an ITER TF coil. The first TFCS for a Japan-manufacturing TF coil completed its fitting test successfully in August 2018, the acceptance test of its WP was completed in August 2018, and then the WP will be cold-tested. Assembly of the TFCS and WP will be started from the fourth quarter of 2018 as the very first ITER TF coil.

## Acknowledgments

suggestions and encouragement during these activities. The authors would also like to acknowledge the contributions of the Toshiba Corporation Power Systems Company for development of the specialized UT technique.

## ORCID iDs

M. Nakahira https://orcid.org/0000-0002-5458-0528

## References

[1] Iguchi M. *et al* 2016 Cryogenic structural materials of the ITER toroidal field coil structure *Proc. of SMINS-4* p IV-1 (http://www.oecd-nea.org/science/smins4/)

[2] Iter Organization 2009 *Design Description Document* (ITER IDM Reference 2MVZNX. version 2.2.)

[3] Ishizaka J., Miura R., Nakajima H. and Shimamoto S. 1990 Strength and toughness of $^{12}$Cr–$^{12}$Ni–$^{10}$Mn–$^{5}$Mo steel for cryogenic structural application *Tetsu-to-Hagane* **76** 149–56

[4] Nakajima H. *et al* 2009 Qualification of cryogenic structural materials for the iter toroidal field coils *Proc. of the ASME 2009 Pressure Vessels and Piping Division Conf. PVP2009-77553* (New York: ASME) pp 1–8

[5] Sakurai T. *et al* 2017 Correlation between the fracture toughness of the austenite stainless steel and martensitic transformation in cryogenic *J. Cryog. Super. Soc. Japan* **52** 260–7

[6] Angel T. 1954 Formation of martensite in austenitic stainless steels *J. Iron Steel Inst.* **177** 165

[7] Nohara K., Ono Y. and Ohashi N. 1977 Composition and grain size dependencies of strain-induced martensitic transformation in metastable austenitic stainless steels *Tetsu-to-Hagane* **63** 772–82

[8] Iguchi M. *et al* 2015 Welding joint design of ITER toroidal field coil structure under cryogenic environment *Proc. of ICONE23* (Tokyo: Japan Society of Mechanical Engineers) p 1713

[9] Iguchi M. *et al* 2012 Development of structures for ITER toroidal field coil in Japan *IEEE Trans. Appl. Supercond.* **22** 4203305

[10] Iguchi M. *et al* 2013 Mechanical properties of full austenitic welding joint at cryogenic temperature for the ITER toroidal field coil structure *Fusion Eng. Des.* **88** 2520–4

[11] Sakurai T. *et al* 2016 Mechanical properties of welded joint at cryogenic temperature for manufacturing of ITER TF coil structure *IEEE Trans. Appl. Supercond.* **26** 4204705

[12] Iguchi M. *et al* 2013 Progress of manufacturing trial for the ITER toroidal field coil structure *IEEE Trans. Appl. Supercond.* **24** 3801004

[13] Iguchi M. *et al* 2018 Progress of ITER TF coil case fabrication in Japan *IEEE Trans. Appl. Supercond.* **28** 4202105

[14] Sakurai T. *et al* 2016 Development of manufacturing technology for ITER TF coil structure *Fusion Eng. Des.* **109** 1592–7